CHEMISTRY
A EUROPEAN JOURNAL

DOI: 10.1002/chem.201000605

Ferrocene-Substituted Dithio-*o*-Carborane Isomers: Influence on the Native Conformation of Myoglobin Protein

Chunhui Wu,[a] Baohua Xu,[b] Juan Zhao,[a] Qibai Jiang,[b] Fadong Wei,[a] Hui Jiang,[a] Xuemei Wang,*[a] and Hong Yan*[b]

Abstract: Biointeractions between two organometallic compounds, a pair of ferrocene-substituted dithio-*o*-carborane isomers ($C_{14}H_{20}B_{10}FeS_2$; denoted as FcSB1 and FcSB2), and myoglobin (Mb) have been investigated by means of electrochemistry, fluorescence, circular dichroism, and UV/Vis absorption spectroscopy. Our observations demonstrate that FcSB1 and FcSB2 could coordinate to the axial position *trans* to the histidine imidazole that induces the change of the heme iron from the high spin state to the low spin state and the changes of the conformation of the aromatic fluorophores of the selected heme protein. Such influences attribute to the structural features of FcSB1 and FcSB2 containing sulfur donor atoms and hydrophobic ferrocenyl and carboranyl units that leads to specific binding modalities with Mb. This study provides an insight into the understanding of relevant biointeractions between the new type of ferrocene–carborane conjugates and hemoproteins, and might shed light on the promising bioapplications of these multifunctional organometallic complexes.

Keywords: biointeractions · bioorganometallic chemistry · carboranes · iron · myoglobin

Introduction

Over the past two decades, the synthesis of new organometallic compounds and investigation of their biomedical effects against various diseases have been the focus for many researchers in bioorganometallic chemistry.[1] Typically, ferrocenyl derivatives have attracted considerable attention.[2] Different types of ferrocenyl derivatives show highly promising activities, such as DNA-cleaving,[3a] antibacterial,[3b] antimalarial,[3c] and anticancer activity.[3d] Owing to the lipophilicity and hydrophicity of the ferrocenyl group, modification of bioactive peptides with a ferrocenyl unit has improved their physicochemical and biological properties.[4] For instance, the ferrocenyl triazole peptide conjugate has demonstrated its ability to reduce its off-rate and to enhance its affinity and antiviral potency for HIV-1 gp120.[4c] As potent pharmaceuticals for breast cancer therapy, ferrocifen (the ferrocenenyl-appended tamoxifen) and its derivatives act by changing the conformation of estrogen receptor proteins (hormone protein) in a noncovalent way and induce DNA damage by the generation of reactive radical species.[2a,5]

On the other hand, carborane derivatives have been extensively involved in areas of drug discovery,[6a] molecular imaging,[6b,c] and targeted radionuclide therapy (i.e. the boron neutron capture therapy (BNCT) for cancer).[6b–d] The hydrophobic character of carboranes could enhance the interactions between pharmaceuticals and their receptors. And their unique three-dimensional structure and synthetic flexibility allow us to probe protein binding in an unprecedented manner, thus tuning the pharmacokinetics of new drug candidates.[6b,c] The reported carborane-containing examples of estrogen agonists,[7a] androgen antagonists,[7b] and transthyretin amyloidosis inhibitors[7c] displayed significant biological activities similar or even superior to those of their nonboronated counterparts. Besides, cobaltacarboranes have been recently identified as potent inhibitors of HIV-1 protease in AIDS therapy.[8]

[a] C. Wu, J. Zhao, F. Wei, Dr. H. Jiang, Prof. X. Wang
State Key Lab of Bioelectronics (Chien-Shiung Wu Lab)
Southeast University, Nanjing
Jiangsu 210096 (China)
Fax: (+86) 025-83792177
E-mail: xuewang@se.edu.cn

[b] Dr. B. Xu, Q. Jiang, Prof. H. Yan
State Key Lab of Coordination Chemistry
School of Chemistry and Chemical Engineering
Nanjing University, Nanjing
Jiangsu 210093 (China)
Fax: (+86) 025-83686724
E-mail: hyan1965@nju.edu.cn

Supporting information for this article is available on the WWW under http://dx.doi.org/10.1002/chem.201000605.

On the basis of the characteristics of ferrocenyl and carboranyl groups, we have explored the biological properties of a new type of molecules conjugated by these two bioactive units through sulfur atoms, denoted as FcSB1 and FcSB2, a pair of geometrical isomers.[9] This paper focuses

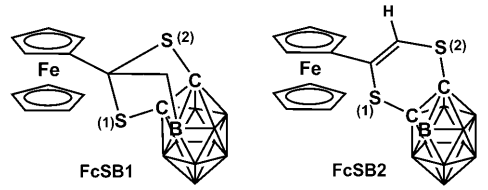

on the description of the biointeractions of the two ferrocene-substituted dithio-*o*-carboranes with the heme protein, myoglobin (Mb). Mb was chosen since it is a very important protein for transporting O_2/CO_2 in living systems and has been well investigated as a typical model protein for biointeractions with various drugs or ligands.[10,11] A cobalt(III) Schiff base complex was found to selectively unfold Mb as a molten globule because of the bond formed between cobalt and an imidazole nitrogen atom of a histidine unit.[11c] In particular, special concern should be directed to the interactions of drugs with blood components, for example, heme proteins, in view of the fact that a vast majority of cytotoxic metal-containing compounds are administered intravenously.[11d,e] The relevant work could be of significance pertaining to the promising bioapplications of these multifunctional organometallic complexes.

Results and Discussion

Electrochemical studies of the interactions between the ferrocene-substituted ditho-*o*-carborane isomers (FcSB1/FcSB2) and Mb: The redox-active ferrocenyl group has been extensively utilized as an electrochemical probe in biomolecular interactions and detections.[12,13] In this study, our investigation indicates that FcSB1 and FcSB2 have good electrochemical properties, thus their interplay with Mb has been probed by electrochemical studies. As shown in Figure 1a and b, the results of the differential pulse voltammetric (DPV) study illustrate that both FcSB1 and FcSB2 could interact strongly with Mb. Upon addition of the protein, dramatic positive shifts in the peak potentials of FcSB1 and FcSB2 occur with the significant decrease of relevant peak currents. The latter attributes to the diffusion of a mixture of the free and protein-bound ferrocene-substituted dithio-*o*-carboranes to the electrode surface.[12e–f,13] In addition, the remarkable positive shifts of the potentials indicate that oxidation of the ferrocenyl groups becomes increasingly difficult.[13a] This clearly reflects the variations in the electronic environment around the ferrocenyl groups. In structure, both FcSB1 and FcSB2 have two electron-rich sulfur atoms[9] and Mb has a weakly bound H_2O or O_2 molecule in

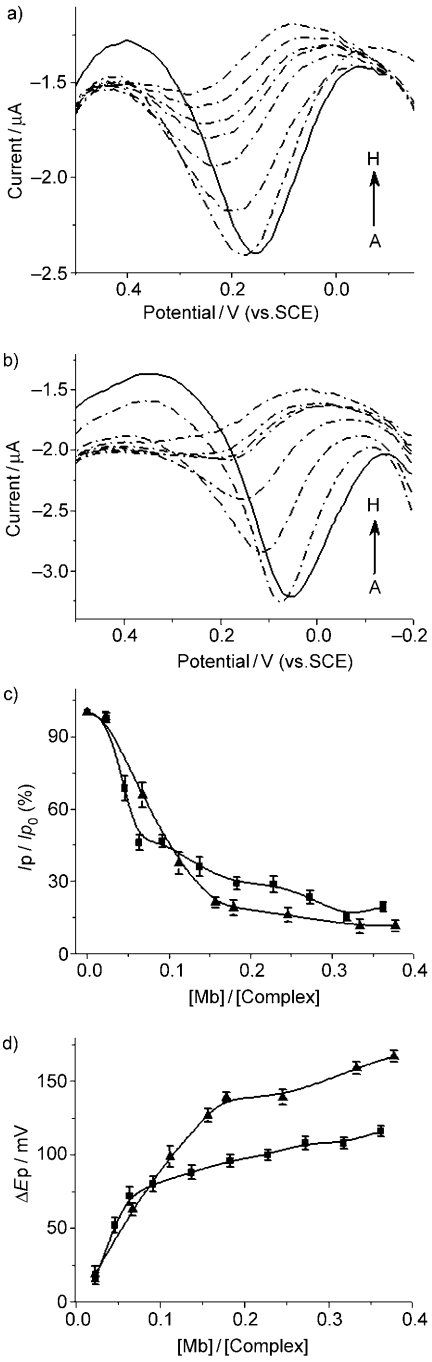

Figure 1. The changes of DPV for FcSB1 (a) and FcSB2 (b) (51.0 μM) in phosphate buffer saline (PBS, 0.02 M, pH 7.40) when titrated with Mb. a) From A to H, [Mb]/[FcSB1] = 0 (——), 0.02, 0.05, 0.09, 0.14, 0.18, 0.27, 0.36. b) From A to H, [Mb]/[FcSB2] = 0 (——), 0.07, 0.11, 0.16, 0.18, 0.25, 0.33, 0.38. Parts c) and d) reflect the peak current (c) and peak potential (d) changes versus different concentration ratios of [Mb]/[complex]. ■: FcSB1, ▲: FcSB2.

its heme iron center at the sixth axial position. Thus, we assume that the sixth coordination position occupied by the H_2O or O_2 molecule has been replaced by one of the two sulfur atoms of the organometallic isomers (see Scheme 1). As a result, the coordination of sulfur to the iron atom of

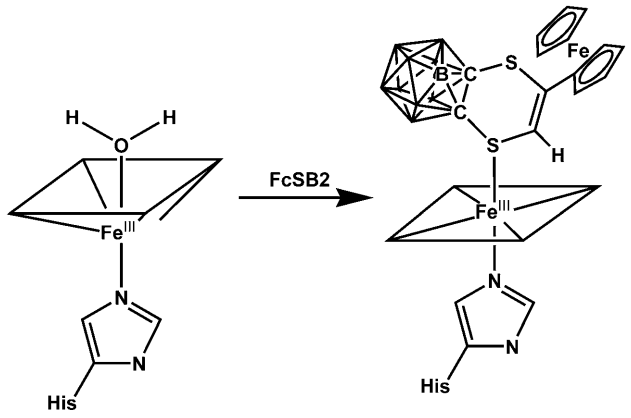

Scheme 1. Schematic presentation of the interaction of Mb with FcSB2.

the heme center decreases the electron density of the adjacent iron center of the ferrocenyl group. This is clearly reflected by the electrochemical studies (Figure 1). Note that the ready replacement of H_2O or O_2 at the sixth coordinative site in Mb and related model complexes coordinated by small sulfur donor ligands and other ligands (i.e. CN^-, N_3^-) has been extensively described.[14]

Figure 1c and d illustrate plots of Ip/Ip_0 and ΔEp of FcSB1 and FcSB2 as a function of protein concentration, respectively. A linear relationship is initially observed and then the curves slowly reach a steady state, indicative of saturation of complexation. For FcSB1, an approximately 120 mV positive shift of peak potential is seen with a decrease to approximately 20% of the peak current at the concentration ratio of [Mb]/[FcSB1] = 0.36, whereas for FcSB2, an approximately 165 mV positive shift of peak potential is observed with the peak current reduced to approximately 12% at [Mb]/[FcSB2] = 0.36. The greater apparent change of the peak potential for FcSB2 indicates a stronger binding to Mb that induces a larger influence on the electronic environment around the ferrocenyl group. This could be explained by their solid-state structures. FcSB1 has a tripod structure with two environmentally equivalent sulfur atoms,[9a] whereas FcSB2 contains a bent six-membered ring with the S(2) atom showing less steric hindrance for coordination.[9b] Moreover, the existence of the vinyl group between the ferrocenyl group and S(2) in FcSB2 should enhance electrochemical alterations. Thus FcSB2 versus FcSB1 has a stronger binding capacity to Mb.

UV/Vis absorption spectroscopic studies of interactions between FcSB1/FcSB2 and Mb: Based on above effective observations, UV/Vis absorption spectroscopy was further utilized to investigate the interactions between the two organometallic isomers and the selected protein to obtain the information on the electronic structure of the heme center. It is well known that Mb has the characteristic bands: one Soret band at around 400 nm and two Q-bands in the range of 500–600 nm, both arising from the π-electron transitions inside the porphyrin ring, and one CT1 band around 630 nm caused by the charge transfer from porphyrin to iron.[15] Upon titration of FcSB1 or FcSB2 to Mb, both lead to red-shifts of the Soret band (i.e. from 408 to 412 nm) and the Q bands (i.e. from 504 to 535 and 535 to 564 nm, respectively) in the same degrees, as well as disappearance of the CT1 band (see Figure 2 and Table 1). These observations reflect that both organometallic compounds can exert a significant effect on the heme center. The isosbestic points at 386 and

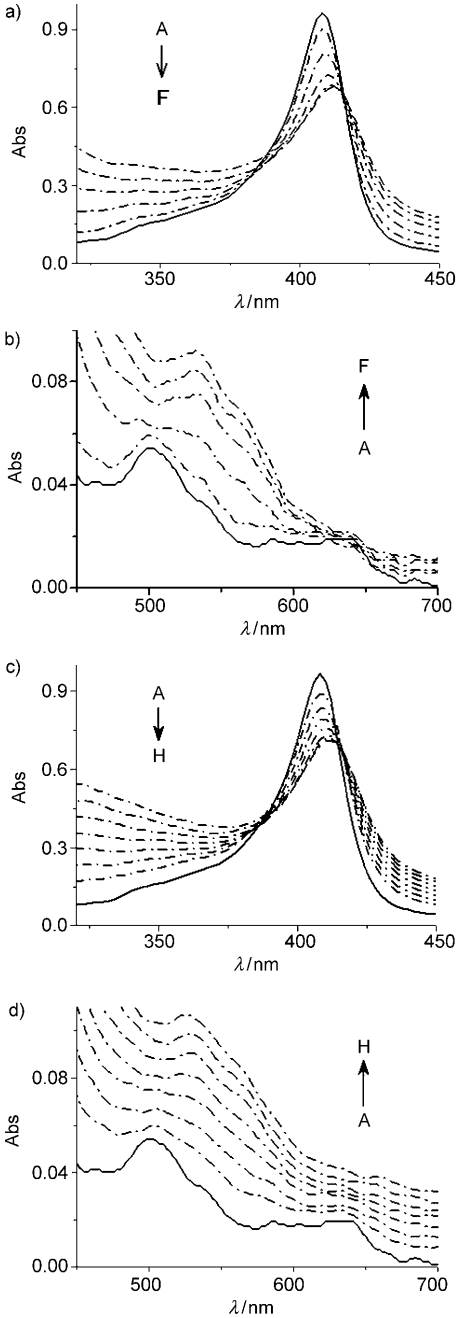

Figure 2. UV/Vis spectral changes of Mb (6.72 μM) in phosphate buffer saline (PBS, 0.02 M, pH 7.40) when titrated with FcSB1 (a and b) and FcSB2 (c and d). a and b) From A to F, [FcSB1]/[Mb] = 0 (——), 2.35, 7.03, 11.7, 16.3, 20.8. c and d) From A to H, [FcSB2]/[Mb] = 0 (——), 3.89, 6.41, 9.58, 12.7, 15.9, 18.9, 22.0.

Table 1. UV/Vis spectral data and Stern–Volmer quenching constants (K_{sv}) of FcSB1 and FcSB2 when binding to Mb.

	Soret band [nm]	Q band [nm]	CT1 band [nm]	$K_b \times 10^3$ [M^{-1}]	$K_{sv} \times 10^3$ [M^{-1}]	$V \times 10^3$ [M^{-1}]
Mb	408	504 535	635			
FcSB1–Mb	412	535 564		7.1 ± 0.3	6.9	7.1
FcSB2–Mb	412	535 564		8.3 ± 0.3	17.0	2.7
BSH–Mb	412	532 561		12.5 ± 0.3		

416 nm indicate the formation of a ground-state complex between Mb and FcSB1 and FcSB2, respectively.

The UV/Vis spectral features depend on the metal oxidation state, peripheral substituents, axial ligands, coordination number, spin state, nearby amino acid residues, etc. As reported in the literature, the intense Soret band (409 nm), Q bands (504 and 535 nm), and the CT1 band (634 nm) in Mb correspond to a six-coordinate high spin state (6-cHS), in which H_2O or O_2 is bound to iron from the opposite direction of the F8-histidine (His-93).[16a] Whereas, the Soret band at 414 nm and Q bands at 535 and 567 nm characterize a six-coordinate low spin state (6-cLS) when a stronger ligand occupies the sixth axial site instead of the weakly bound H_2O or O_2.[16b,c] Thus, the similar spectral changes of Mb upon binding to FcSB1 or FcSB2 demonstrate that both compounds can induce the spin-state change of the heme iron atom from 6-cHS to 6-cLS. Obviously, this results from sulfur donor atom replacement of H_2O or O_2. In addition, the Fe–S axial coordination has occurred in a number of heme proteins (e.g. cytochrome c[17a] and cytochrome P-450[17b]) and enzymes (e.g. chloroperoxidase[17b] and nitric oxide synthase[17c]). Binding of exdogenous sulfur donor ligands (i.e. thiol, thiolate, thioether and disulfide) to the heme centers of cytochrome P-450-CAM and Mb have also been reported.[14a,b]

Furthermore, the apparent binding constants K_b were calculated (see Equation S1 in the Supporting Information)[18] and listed in Table 1. The values of the apparent binding constants obtained here for the two organometallic species to the selected protein show that FcSB2 has a stronger affinity to the heme iron center, parallel to the electrochemical studies. This might be attributed to the decreased steric hindrance around the S(2) donor atom in FcSB2 relative to that in FcSB1, which makes its coordination to iron more favorable. To further verify the steric influence of the ferrocenyl group on the coordination capability in FcSB1 and FcSB2, dithio-*o*-carborane (denoted as BSH, see Scheme S1 in the Supporting Information) was tested for comparison. Indeed, the result shows that BSH has a larger binding constant to Mb (see Table 1 and Figure S1a in the Supporting Information). Additionally, *o*-carborane was also tested, and no effect on the relevant spectrum of the target protein was found (data not shown). Hence, there is no doubt that FcSB1 and FcSB2 serve as metal ligands to competitively bind to the heme iron center of Mb via the electron-rich dithio units.

Circular dichroism (CD) spectroscopic studies of the effect of FcSB1/FcSB2 on Mb: To further investigate the effect of ferrocene–carborane conjugates on Mb, the CD spectra were explored. CD is a sensitive technique to monitor the conformational changes of proteins upon their interaction with ligands. It is well-known that Mb has three distinct regions in the CD spectrum (see Figure S2 in the Supporting Information). The far-UV region (from 190 to 240 nm) correlates with the secondary structure of the macromolecule, that is, α-helix, parallel and antiparallel β-sheet, β-turn, and no ordered region content.[19a] The near-UV region (from 240 to 300 nm) originates from the aromatic amino acid side chains, which gives detailed information on ''local'' chain–chain interactions.[19a,b] In the visible region, the Soret CD spectrum of Mb (~400 nm) results from the interactions between the π–π* transition of the heme chromophore and the surrounding aromatic amino acids. It is greatly influenced by the orientation of the aromatic amino acid residues with respect to the heme, and the positions of these residues in the primary structure.[19c,d] Thus, the change of the Soret CD spectrum shows the variations not only in the electronic state of the heme, but also in its microenvironment.[19e]

Upon addition of FcSB1 or FcSB2, the relevant CD bands of Mb display obvious variations as shown in Figure 3. In comparison, the isomers do not exhibit any CD bands. The Soret CD signal at 408 nm for Mb is gradually diminished with the increasing of the concentration of FcSB1 or FcSB2 (Figure 3a and b, respectively), which indicates that the Mb protein matrix is gradually unfolded.[20a,b] Finally, the characteristic Soret CD bands of Mb completely disappear when the ratio of [FcSB1]/[Mb] and [FcSB2]/[Mb] reaches 19.6 and 14.5, respectively. Figure 3c shows the unfolding percentage as a function of the concentration ratio; it is observed that FcSB2 has a stronger unfolding effect on the heme protein than FcSB1. The Soret CD band directly relates to the molecular structures around the heme prosthetic groups, which are sensitive to the changes in the quaternary and tertiary structures of the hemoproteins.[20b,c] Clearly, the heme environment of Mb is profoundly affected by the ferrocene–carborane conjugates as observed by the remarkable change of the Soret CD band. In Mb, the heme prosthetic group is totally buried in a hydrophobic cleft formed by helixes A to H. Hydrophobic interactions between the tetrapyrrole ring and the hydrophobic amino acid groups on the interior of the cleft could strongly stabilize the heme protein conjugates.[11a] FcSB1 and FcSB2 could easily gain access to the heme pocket owing to their hydrophobic properties. The electron-rich dithio groups of the isomers can readily replace H_2O and coordinate to the heme iron center at the sixth axial position (see Scheme 1).

Additionally, both FcSB1 and FcSB2 can also exert an influence on the near-UV CD bands. For example, at a ratio

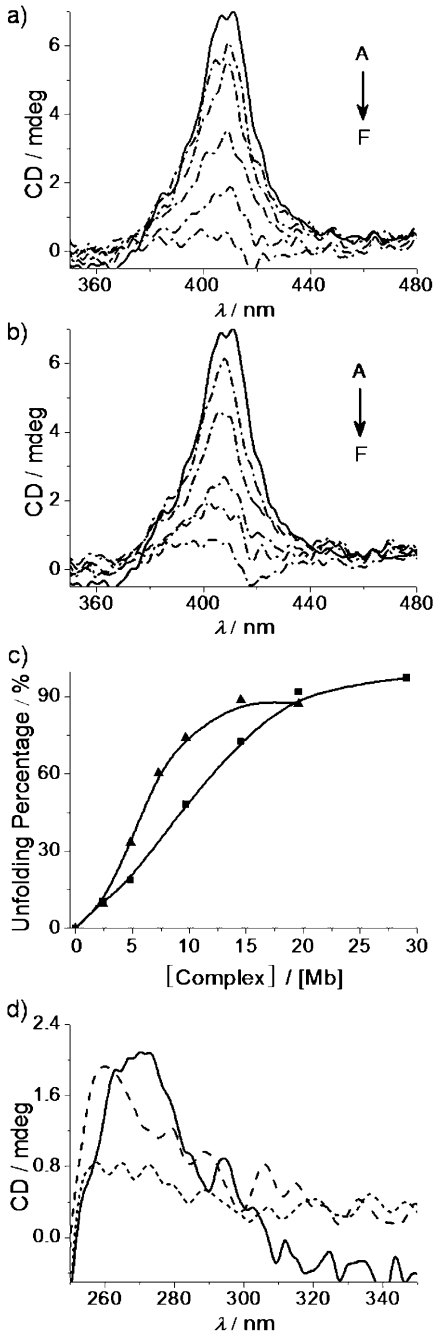

Figure 3. The visible CD spectra of Mb (6.72 μM) in PBS (0.02 M, pH 7.40) containing DMSO ($V_{DMSO}/V_{PBS}=0.24\%$) after interacting with FcSB1 (a) and FcSB2 (b). a) From A to F, [FcSB1]/[Mb] = 0 (——), 2.4, 4.8, 9.7, 14.5, 19.6. b) From A to F, [FcSB2]/[Mb] = 0 (——), 2.4, 4.8, 7.3, 9.7, 14.5. c) Illustration of the unfolding profile of Mb interacting with FcSB1 (■) and FcSB2 (▲). d) The near-UV CD of Mb (——) after interacting with FcSB1 (– – –; 132 μM) and FcSB2 (-----; 97 μM).

of 14.5:1 for [FcSB2]/[Mb], virtually no CD signal could be observed, as shown in Figure 3d. The loss of the near-UV bands indicates the diminished packing around the aromatic amino acids.[11c] It is reported that the near-UV CD bands at 270 nm could be assigned to electronic transitions in tryptophans (Trp) and tyrosines (Tyr),[21] probing the tertiary structure of Mb only in the AGH domain. Thus above observations suggest that the tertiary fold in the AGH domain may smear out upon addition of these organometallic compounds. The detailed effect of the isomers on the aromatic groups can be further explored by fluorescence experiments. In fact, the secondary structural transitions can be easily studied by the far-UV CD (190–250 nm) spectrum, for example, the decrease of ellipticity at 222 nm (i.e. the ellipticity is decreased by 16 and 22% for FcSB1 and FcSB2 at the [complex]/[Mb] ratio = 9.7, respectively; see Figure S3 in the Supporting Information) demonstrates that the secondary structure is slightly affected. However, the effect of the higher concentration of isomers cannot be detected owing to the extremely high absorbance of DMSO solvent in this region.

Fluorescence investigation on the protein-binding behavior of FcSB1 and FcSB2: The intrinsic fluorescence of proteins originates from the Trp and Tyr fluorophores and is sensitive to the microenvironment of the amino acid residues. Changes in emission spectra are in response to protein conformational transitions, subunit association, substrate binding, or denaturation.[22] Besides, fluorescence measurements can give information on the binding of small molecules to proteins on a molecular level, such as binding mechanism, binding constant, and binding mode.

In the present study, the effect of nonfluorescent FcSB1 and FcSB2 on the fluorescence of Mb was explored. As shown in Figure 4, both FcSB1 and FcSB2 (Figure 4a and b, respectively) significantly decrease the fluorescence intensity (FI) of Mb, accompanied with the progressive redshift of the emission peak, that is, up to 10 nm for FcSB1 and 25 nm for FcSB2. This phenomenon suggests that the fluorophore residues in Mb have been moved away from the heme owing to incorporation of the organometallic species and become more exposed to the solvent.[16b] Figure 4c shows the quenching comparisons of Mb fluorescence by the two isomers, and it can be seen that FcSB2 versus FcSB1 displays a stronger quenching effect. Clearly, this is caused by the structural differences of the isomers that lead to the interactions with the fluorophore residues in different degrees. Similar enhanced fluorescence quenching phenomena have also occurred in other ferrocene-containing conjugates.[13c]

Two types of fluorescence quenching are present, that is, dynamic and static quenching. The former is caused by collision between a fluorescence substance and a quencher, whereas the latter is attributed to the formation of a ground-state complex between a fluorophore molecule and a quencher.[23a] In many cases, both quenching types are present. To discover the quenching mechanism in our system by FcSB1 and FcSB2, the data have been analyzed by using the Stern–Volmer equation (see Equation S2 in the Supporting Information),[23b] and the upward curvature curves were obtained as shown in Figure 4d. This equation reveals a characteristic plot of combined quenching mechanisms, that is, both the static and the dynamic types.[23c–e] The static quenching constant V and the dynamic quenching

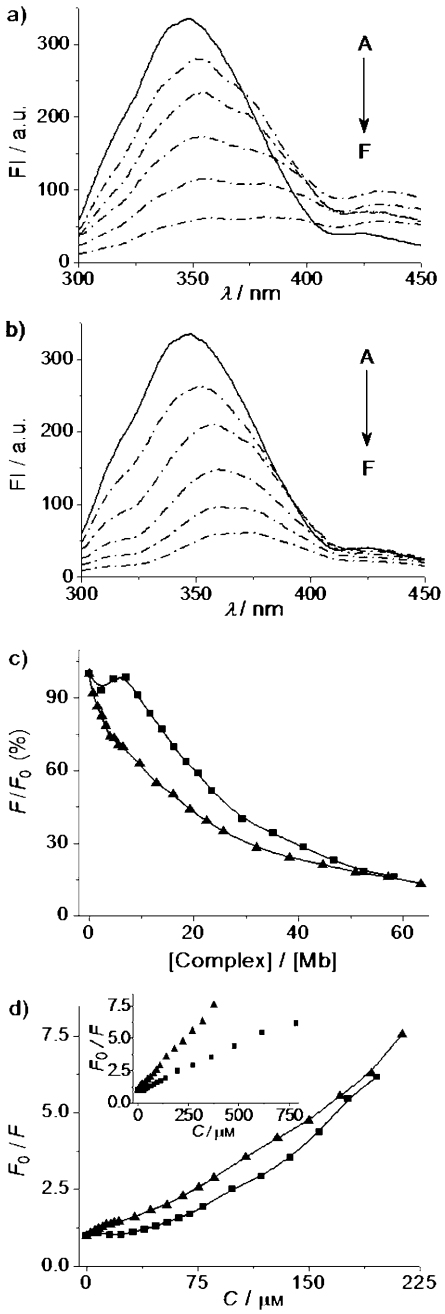

Figure 4. Fluorescent spectral changes of Mb (3.36 μM) in PBS (0.02 M, pH 7.40) when titrated with FcSB1 (a) and FcSB2 (b). a) From A to F, [FcSB1]/[Mb] = 0 (——), 11.7, 16.3, 23.5, 35.2, 52.6. b) From A to F, [FcSB2]/[Mb] = 0 (——), 3.22, 9.67, 19.3, 32.0, 50.9. c) The quenching comparisons of Mb fluorescence by FcSB1 (■) and FcSB2 (▲). d) The Stern–Volmer curves and modified Stern–Volmer curves (inset) with FcSB1 (■) and FcSB2 (▲) binding to Mb.

constant K_{sv} were further calculated from the slopes (inset in Figure 4d; see Equation S3 in the Supporting Information).[23f] Both values are presented in Table 1, and the data show that FcSB1 quenches the fluorescence of Mb with a nearly equal static and dynamic quenching constant. Whereas for FcSB2, the apparent difference between the values of K_{sv} and V indicates that the quenching is dominated by the dynamic quenching type.

Several types of forces could be responsible for the fluorescent changes when a ligand interacts with a protein, for instance, chemical bonds, hydrogen bonding, electrostatic, van der Waals forces, hydrophobic, and hydrophilic interactions.[24] From the structural characteristics of the two isomers and the target protein, hydrophobic interactions would be predominant, and electrostatic interactions are weak since FcSB1 and FcSB2 are neutral and Mb is almost electrically neutral at pH 7.4 (isoelectric point of 7.2[25]). The hydrophobic groups of the ferrocenyl and carboranyl units in the two organometallic compounds could more easily interact with the monomeric Mb matrix through hydrophobic interactions with the nonpolar parts of the surface and the interior of the protein. Besides, the "nick" S atoms in both FcSB1 and FcSB2 are ready to generate intermolecular hydrogen bonding with Mb, which may also contribute to the fluorescent changes.

Synchronous fluorescence spectroscopic studies of the influence of FcSB1/FcSB2 on the aromatic residues: Synchronous fluorescence spectroscopy (SFS) was further utilized to explore the effect of FcSB1 and FcSB2 on the microenviroments in a vicinity of the aromatic residues of Mb. Since the SFS technique involves simultaneous scanning of the excitation and emission monochromators while maintaining a constant wavelength interval, it can identify the overlapped excitation peaks of Trp and Tyr residues of proteins.[26a] If $\Delta\lambda$ between excitation and emission wavelengths is used at 15 and 60 nm, SFS can give the characteristic information on the individual Tyr and Trp residues.[26b] The shifts in the maximum emission wavelength of the Trp and Tyr residues correspond to the changes in polarity around the chromosphere molecules. The redshift suggests that the aromatic residues buried in nonpolar hydrophobic cavities have moved to a more hydrophilic environment, whereas the blueshift signifies the enhancement of hydrophobicity.[20a,27] As shown in Figure 5a and b, upon addition of FcSB1, the maximum emission wavelengths of both Trp and Tyr residues are shifted to red by approximately 10 nm. This reflects the increased polarity around the Trp and Tyr residues (i.e. the two aromatic residues are moved into a more hydrophilic environment) and the decreased hydrophobicity.[20a,27] However, after addition of FcSB2, the peak of the Trp residues has a redshift of approximately 6 nm (Figure 5c), whereas the peak of the Tyr residues is shifted to blue by approximately 12 nm (Figure 5d). These observations also demonstrate the conformational changes surrounding the Tyr and Trp residues. Similarly, the redshift of the Trp residues corresponds to the increased polarity around the residues, hence the decreased hydrophobicity. Whereas, the blueshift of the Tyr residues displays the decreased polarity around the residues and the increased hydrophobicity.[28]

It is known that two types of Trp residues are present in helix A in Mb, one is located at the 7th position (Trp-7) and exposed to water, whereas the other is located at the 14th

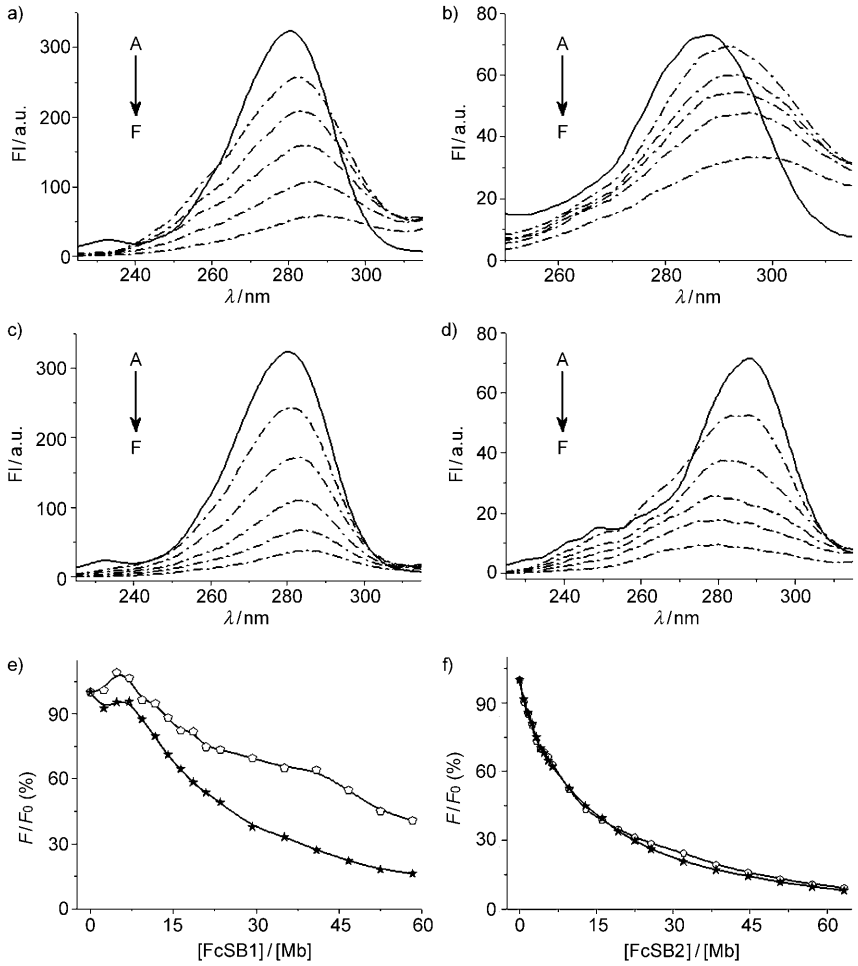

Figure 5. Synchronous fluorescence spectral changes of Mb (3.36 μM) in PBS (0.02 M, pH 7.40) when titrated with FcSB1 (a and b) and FcSB2 (c and d). a and b) From A to F, [FcSB1]/[Mb] = 0 (——), 11.7, 16.3, 23.5, 35.2, 52.6. c and d) From A to F, [FcSB2]/[Mb] = 0 (——), 3.22, 9.67, 19.3, 32.0, 50.9. e and f) The quenching comparisons of Mb synchronous fluorescence caused by FcSB1 (e) and FcSB2 (f). ★: Trp residues, ○: Tyr residues. For a) and c), $\Delta\lambda = 60$ nm for Trp residues. For b) and d), $\Delta\lambda = 15$ nm for Tyr residues.

position (Trp-14) and buried under the hydrophobic protein matrix.[29a] The Tyr-103 and Tyr-146 of Mb are located in helixes G and H, respectively.[29b] Therefore, our observations imply the rearrangement of the tertiary structure in the surrounding of Trp and Tyr residues in the helixes A, G, and H owing to the incorporation of FcSB1 and FcSB2. FcSB1 is possibly situated closer to the Trp residues since the FI of the Trp residues decreases faster than that of the Tyr residues (Figure 5e), and FcSB2 may be equally close to both Trp and Trp residues since their FIs decrease by a nearly equal degree (Figure 5f).

Conclusion

In summary, we have studied the interactions between the two ferrocene-substituted dithio-*o*-carboranes, FcSB1 and FcSB2, and the heme protein myoglobin. The investigations from electrochemistry, UV/Vis absorption, and CD spectroscopy demonstrate that these ferrocene–carborane conjugates could bind to the heme iron center through the replacement of the weakly bound H_2O/O_2 in the distal heme pocket by their electron-rich sulfur donors. The metal complexes also lead to the change of the spin state of the heme iron atom, that is, from a six-coordinate high spin state to a six-coordinate low spin state. The tertiary structure of myoglobin, especially the native heme environment is substantially disrupted as demonstrated by the change of the Soret CD band. Moreover, introduction of these organometallic species can alter the microenvironment around the Trp and Tyr fluorophores, thus quenching the fluorescence of the target protein owing to the change in polarity, hydrophobic interactions and hydrogen bonding, and so on. The structural differences of the two organometallic isomers lead to different performances when interacted with Mb as revealed by the techniques used. Thus, studies on the protein-binding behavior of the ferrocene–carborane conjugates, such as FcSB1 and FcSB2, containing multifunctional groups would give meaningful insights on the evaluation of their promising biomedical applications and the benefits of the development of potential multifunctional metallodrugs.

Experimental Section

Reagents: Compounds FcSB1, FcSB2, and dithio-*o*-carborane (BSH) were synthesized according to the literature.[9,30] Myoglobin from equine skeletal muscle (methemoglobin) was purchased from Sigma and used without further purification. The Mb protein was dissolved in PBS (0.02 M, pH 7.40) with doubly distilled water. The concentration of Mb was determined spectrophotometrically according to the molar absorption coefficient $\varepsilon = 157000\ L\,cm^{-1}\,mol^{-1}$ at 406 nm respectively. Solutions prepared in this way were used as the protein native state. The other reagents used were of analytical grade. The stock solutions of FcSB1, FcSB2, and BSH were prepared in DMSO with concentrations of 22.2 mM, 54.3 mM, and 0.12 M, respectively. The stock solution of *o*-carborane ($C_2B_{10}H_{12}$) was prepared in DMSO with a concentration of 61.0 mM.

Electrochemical studies: DPV studies were performed on a CHI660b electrochemical workstation. All measurements were carried out at ambient temperature (22 ± 2 °C) under the nitrogen environment in a three-component electrochemical cell consisting of a glassy-carbon electrode as

the working electrode, a Pt wire as the counter-electrode and a saturated calomel electrode SCE as the reference electrode. Pulse amplitude: 0.05 V, pulse width: 0.05 s, pulse period: 0.1 s. A 2.5 mL diluted PBS (0.02 M, pH 7.40) solution of FcSB1 (51.0 μM) and FcSB2 (51.0 μM) in an electrochemical cell were kept constant while varying the concentration of Mb in solution. Aliquots of a known volume of Mb (1.22 mM) were added. The solutions were kept for 5 min before measurement. Prior to every electrochemical assay, the GCE was polished to a mirrorlike surface with 0.05 μm Al_2O_3, then sonicated in water for 5 min to carry out the electrochemical detection.

UV/Vis absorption spectroscopic studies: The UV/Vis absorption spectroscopic study was performed on a U-4100 (HITACHI) spectrometer. Absorption spectra were recorded between 300–700 nm. The data interval was 2 nm. Titrations were carried out by keeping the concentration of Mb constant, while varying the concentration of compounds (FcSB1, FcSB2, BSH, and *o*-carborane). A 2.5 mL solution of PBS (0.02 M, pH 7.40) in a septum-capped quartz cuvette (1 cm path length), containing Mb (6.72 μM), was titrated by successive additions of the appropriate diluted solution of carborane compound. Titrations were carried out manually by using trace syringes. In the titration process, the total added volume was kept to less than 50 μL. The solutions were allowed to equilibrate for 5 min before measurements. The spectrum was recorded after each addition. The control experimental results show that the maximum concentration of DMSO used ($V_{DMSO}/V_{PBS}=2.4\,\%$) has little effect on the UV/Vis absorption spectrum of the Mb protein (see Figure S1b in the Supporting Information).

CD spectroscopic studies: CD measurements were performed on a JASC0–810 CD spectropolarimeter. The protein concentration used was 6.72 μM in PBS (0.02 M, pH 7.40) containing DMSO ($V_{DMSO}/V_{PBS}=0.24\,\%$), and the curettes of 0.1 cm path length were used in the far-UV (190–240 nm) region and 1.0 cm path length in the near-UV (240–340 nm) and visible regions (340–550 nm), respectively. The spectropolarimeter was sufficiently purged with 99.9 % dry nitrogen before starting the instrument. Photomultiplier absorbance did not exceed 600 V in the spectral regions measured. All the measurements were performed at room temperature ($22\pm2\,^{\circ}C$) under a nitrogen flow ($3\,L\,h^{-1}$). The spectra were collected at a scan speed of $100\,nm\,min^{-1}$ and a response time of 1 s. Each spectrum was signal-averaged two times, and baseline-corrected by subtracting the buffer spectrum containing DMSO ($V_{DMSO}/V_{PBS}=0.24\,\%$). The unfolding percentage of Mb is calculated as follows: $(1-(\theta/\theta_0))\times100\,\%$, in which θ and θ_0 are the ellipticity of the Soret CD band of Mb in the presence and absence of FcSB1 and FcSB2, respectively.

Fluorescence and synchronous fluorescence spectroscopic studies: Fluorescence spectra were measured on a Perkin–Elmer LS50B spectrofluorimeter at room temperature ($22\pm2\,^{\circ}C$). The slit width is 10.0 nm for both the excitation and emission monochromators. The excited wavelengths were 280 nm. The synchronous fluorescence spectra were recorded in the "both scan" mode in which both excitation and emission monochromators move simultaneously at a fixed difference between excitation and emission wavelength (15 and 60 nm). The data were presented as the average of three scan in all cases. Titrations were carried out by keeping the concentration of Mb constant, while varying the concentration of complexes (FcSB1 and FcSB2). A 2.5 mL solution of PBS (0.02 M, pH 7.40) in a septum-capped quartz cuvette (1 cm path length), containing Mb (3.36 μM), was titrated by successive additions of the appropriate diluted solution of FcSB1 and FcSB2. Titrations were done manually by using trace syringes. And in the titration process, the total added volume was kept to less than 50 μL. The control experimental results show that the maximum concentration of DMSO used ($V_{DMSO}/V_{PBS}=2.0\,\%$) has little effect on the fluorescence and synchronous fluorescence spectra of the Mb protein (see Figure S4 in the Supporting Information).

Fluorescence quenching study: Fluorescence quenching is the decrease of the quantum yield of fluorescence from a fluorophore induced by a variety of molecular interactions with quencher molecule. Quenching may result from a variety of processes, such as excited-state reactions, molecule rearrangement, energy transfers, ground-state complex formation, and collisional processes.[23b] Quenching types often include static and dynamic quenching. The dynamic quenching is when the fluorescence substance collides with quencher, which brings about a decrease of quantum yield and fluorescence strength. Static quenching is due to the formation of a ground-state complex between fluorophore and quencher.[23a] In many instances, the fluorophore can be quenched both by collision and by complex formation with the same quencher. The quenching type could be differentiated from the Stern–Volmer (SV) plot derived from the equation:[23b] $F_0/F=1+K_{sv}\times[Q]$, in which F_0 and F denote the steady-state fluorescence intensity in the absence and presence of quencher, respectively. K_{sv} is the SV quenching constant and $[Q]$ is the concentration of the quencher. Within certain concentrations, the Stern–Volmer curve would be linear if the quenching type is single static or dynamic quenching.[23b,c] If the quenching is combined by both static and dynamic types, the Stern–Volmer plot becomes an upward curvature.[23d,e] In the case of both the dynamic and static quenching mechanism, the fluorescence data can be analyzed by the following modified SV equation:[23f] $F_0/F=1+K_{sv}\times[Q]\times\exp(V[Q])$, in which V is the static quenching constant and could be obtained from the equation by plotting (F_0/F) versus ($[Q]\times\exp(V[Q])$ by varying V until a linear plot was acquired. K_{sv} could then be obtained from the slope.

Acknowledgements

The research is supported by the National Natural Science Foundation of China (90713023, 20675014, 20721002, 20925104), the National High Technology Research and Development Program of China (2007AA022007), a Doctoral Fund from the Ministry of Education of China (20090092110028), the National Basic Research Program of China (2010CB732404, 2007CB925101, 2010CB923303), and the Natural Science Foundation of Jiangsu Province (BK2008149) and Visiting Scholar Foundation of Key laboratory of Biorheological Science and Technology (Chongqing University), Ministry of Education, State Key Laboratory of Coordination Chemistry, Nanjing University, State Key Laboratory of Electroanalytical Chemistry, Changchun Institute of Applied Chemistry Chinese Academy of Science. C.W. acknowledges support by the Graduate Research and Innovation Program of Jiangsu Province (CX07B 177z).

[1] a) C. G. Hartinger, P. J. Dyson, *Chem. Soc. Rev.* **2009**, *38*, 391–401; b) R. H. Fish, G. Jaouen, *Organometallics* **2003**, *22*, 2166–2177.

[2] a) M. F. R. Fouda, M. M. Abd-Elzaher, R. A. Abdelsamaia, A. A. Labib, *Appl. Organomet. Chem.* **2007**, *21*, 613–625; b) D. R. van Staveren, N. Metzler-Nolte, *Chem. Rev.* **2004**, *104*, 5931–5985.

[3] a) Y. N. Vashisht Gopal, D. Jayaraju, A. K. Kondapi, *Arch. Biochem. Biophys.* **2000**, *376*, 229–235; b) J. T. Chantson, M. V. Verga Falzacappa, S. Crovella, N. Metzler-Nolte, *ChemMedChem* **2006**, *1*, 1268–1274; c) C. Biot, G. Glorian, L. A. Maciejewski, J. S. Brocard, O. Domarle, G. Blampain, P. Millet, A. J. Georges, H. Abessolo, D. Dive, J. Lebibi, *J. Med. Chem.* **1997**, *40*, 3715–3718; d) O. Buriez, J. M. Heldt, E. Labbé, A. Vessières, G. Jaouen, C. Amatore, *Chem. Eur. J.* **2008**, *14*, 8195–8203.

[4] a) A. Pinto, U. Hoffmanns, M. Ott, G. Fricker, N. Metzler-Nolte, *ChemBioChem* **2009**, *10*, 1852–1860; b) F. Noor, R. Kinscherf, G. A. Bonaterra, S. Walczak, S. Wölfl, N. Metzler-Nolte, *ChemBioChem* **2009**, *10*, 493–502; c) H. Gopi, S. Cocklin, V. Pirrone, K. McFadden, F. Tuzer, I. Zentner, S. Ajith, S. Baxter, N. Jawanda, F. C. Krebs, I. M. Chaiken, *J. Mol. Recognit.* **2009**, *22*, 169–174.

[5] a) S. Top, A. Vessières, G. Leclercq, J. Quivy, J. Tang, J. Vaissermann, M. Huché, G. Jaouen, *Chem. Eur. J.* **2003**, *9*, 5223–5236; b) A. Vessirès, S. Top, P. Pigeon, E. A. Hillard, L. Boubeker, D. Spera, G. Jaouen, *J. Med. Chem.* **2005**, *48*, 3937–3940; c) E. Hillard, A. Vessières, S. Top, P. Pigeon, K. Kowalski, M. Huché, G. Jaouen, *J. Organomet. Chem.* **2007**, *692*, 1315–1326.

[6] a) J. F. Valliant, K. J. Guenther, A. S. King, P. Morel, P. Schaffer, O. O. Sogbein, K. A. Stephenson, *Coord. Chem. Rev.* **2002**, *232*, 173–230; b) V. I. Bregadze, I. B. Sivaev, S. A. Glazun, *Anti-Cancer Agents Med. Chem.* **2006**, *6*, 75–109; c) A. F. Armstrong, J. F. Val-

liant, *Dalton Trans.* **2007**, 4240–4251; d) A. H. Soloway, W. Tjarks, B. A. Barnum, F. G. Rong, R. F. Barth, I. M. Codogni, J. G. Wilson, *Chem. Rev.* **1998**, *98*, 1515–1562.

[7] a) Y. Endo, T. Iijima, Y. Yamakoshi, H. Fukasawa, C. Miyaura, M. Inada, A. Kubo, A. Itai, *Chem. Biol.* **2001**, *8*, 341–355; b) S. Fujii, T. Goto, K. Ohta, Y. Hashimoto, T. Suzuki, S. Ohta, Y. Endo, *J. Med. Chem.* **2005**, *48*, 4654–4662; c) R. L. Julius, O. K. Farha, J. Chiang, L. J. Perry, M. F. Hawthorne, *Proc. Natl. Acad. Sci. USA* **2007**, *104*, 4808–4813.

[8] a) P. Cígler, M. Kožíšek, P. Řezáčová, J. Brynda, Z. Otwinowski, J. Pokorná, J. Plešek, B. Grüner, L. Dolečková-Marešová, M. Máša, J. Sedláček, J. Bodem, H. G. Kräusslich, V. Král, J. Konvalinka, *Proc. Natl. Acad. Sci. USA* **2005**, *102*, 15394–15399; b) M. Kožíšek, P. Cígler, M. Lepšík, J. Fanfrlík, P. Řezáčová, J. Brynda, J. Pokorná, J. Plešek, B. Grüner, K. Grantz Šašková, J. Václavíková, V. Král, J. Konvalinka, *J. Med. Chem.* **2008**, *51*, 4839–4843.

[9] a) B. H. Xu, X. Q. Peng, Y. Z. Li , H. Yan, *Chem. Eur. J.* **2008**, *14*, 9347–9356; b) B. H. Xu, X. Q. Peng, Z. W. Xu, Y. Z. Li , H. Yan, *Inorg. Chem.* **2008**, *47*, 7928–7933.

[10] a) B. A. Springer, S. G. Sligar, J. S. Olson, G. N. Phillips, Jr., *Chem. Rev.* **1994**, *94*, 699–714; b) G. N. Phillips, Jr., B. M. Pettitt, *Protein Sci.* **1995**, *4*, 149–158; c) Z. Gryczynski, J. Lubkowski, E. Bucci, *J. Biol. Chem.* **1995**, *270*, 19232–19237.

[11] a) P. Taboada, Y. Fernández, V. Mosquera, *Biomacromolecules* **2004**, *5*, 2201–2211; b) M. A. Cheema, P. Taboada, S. Barbosa, E. Castro, M. Siddiq, V. Mosquera, *J. Phys. Chem. B* **2007**, *111*, 13851–13857; c) O. Blum, A. Haiek, D. Cwikel, Z. Dori, T. J. Meade, H. B. Gray, *Proc. Natl. Acad. Sci. USA* **1998**, *95*, 6659–6662; d) A. S. Chakraborti, *Mol. Cell. Biochem.* **2003**, *253*, 49–54; e) A. R. Timerbaev, C. G. Hartinger, S. S. Aleksenko, B. K. Keppler, *Chem. Rev.* **2006**, *106*, 2224–2248.

[12] a) F. Patolsky, Y. Weizmann, I. Willner, *J. Am. Chem. Soc.* **2002**, *124*, 770–772; b) A. Lataifeh, S. Beheshti, H. B. Kraatz, *Eur. J. Inorg. Chem.* **2009**, 3205–3218; c) P. Molina, A. Tárraga, A. Caballero, *Eur. J. Inorg. Chem.* **2008**, 3401–3417; d) Y. L. Zhang, P. F. Pang, J. H. Jiang, G. L. Shen, R. Q. Yu, *Electroanalysis* **2009**, *21*, 1327–1333; e) Y. Peng, Y. N. Liu, F. M. Zhou, *Electroanalysis* **2009**, *21*, 1848–1854; f) J. M. Casas-Solvas, E. Ortiz-Salmerón, J. J. Giménez-Martínez, L. García-Fuentes, L. F. Capitán-Vallvey, F. Santoyo-González, A. Vargas-Berenguel, *Chem. Eur. J.* **2009**, *15*, 710–725.

[13] a) K. A. Mahmoud, H. B. Kraatz, *Chem. Eur. J.* **2007**, *13*, 5885–5895; b) M. Ravera, S. Baracco, C. Cassino, D. Colangelo, G. Bagni, G. Sava, D. Osella, *J. Inorg. Biochem.* **2004**, *98*, 984–990; c) K. K. W. Lo, J. S. Y. Lau, N. Y. Zhu, *New J. Chem.* **2006**, *30*, 1567–1575.

[14] a) M. Sono, L. A. Andersson, J. H. Dawson, *J. Biol. Chem.* **1982**, *257*, 8308–8320; b) C. R. E. Jefcoatet, J. L. Gaylor, *Biochemistry* **1969**, *8*, 3464–3472; c) M. Sono, J. H. Dawson, *J. Biol. Chem.* **1982**, *257*, 5496–5502.

[15] a) F. Cataldo, L. Gentilini, *Polym. Degrad. Stab.* **2005**, *89*, 527–533; b) F. Neri, D. Kok, M. A. Miller, G. Smulevich, *Biochemistry* **1997**, *36*, 8947–8953.

[16] a) W. A. Eaton, R. M. Hochstrasser, *J. Chem. Phys.* **1968**, *49*, 985–995; b) L. Tofani, A. Feis, R. E. Snoke, D. Berti, P. Baglioni, G. Smulevich, *Biophys. J.* **2004**, *87*, 1186–1195; c) P. Strittmatter, S. F. Velick, *J. Biol. Chem.* **1956**, *221*, 253–264.

[17] a) I. Rasnik, K. A. Sharp, J. A. Fee, J. M. Vanderkooi, *J. Phys. Chem. B* **2001**, *105*, 282–286; b) J. H. Dawson, *Science* **1988**, *240*, 433–439; c) K. Szaciłowski, A. Chmura, Z. Stasicka, *Coord. Chem. Rev.* **2005**, *249*, 2408–2436.

[18] S. Maitra, B. Saha, C. R. Santra, A. Mukherjee, S. Goswami, P. K. Chanda, P. Karmakar, *Int. J. Biol. Macromol.* **2007**, *41*, 23–29.

[19] a) E. Bismuto, F. Mancinelli, G. ďAmbrosio, R. Massa, *Eur. Biophys. J.* **2003**, *32*, 628–634; b) N. A. Nicola, E. Minasian, C. A. Appleby, S. J. Leach, *Biochemistry* **1975**, *14*, 5141–5149; c) M. C. Hsu, R. W. Woody, *J. Am. Chem. Soc.* **1971**, *93*, 3515–3525; d) M. C. Hsu, R. W. Woody, *J. Am. Chem. Soc.* **1969**, *91*, 3679–3681; e) K. Mawatari, S. Matsukawa, Y. Yoneyama, *Biochim. Biophys. Acta Protein Struct. Mol. Enzymol.* **1983**, *745*, 219–228.

[20] a) C. W. Liu, A. L. Bo, G. J. Cheng, X. Q. Lin, S. J. Dong, *Biochim. Biophys. Acta Protein Struct. Mol. Enzymol.* **1998**, *1385*, 53–60; b) T. Ferri, A. Poscia, F. Ascoli, R. Santucci, *Biochim. Biophys. Acta Protein Struct. Mol. Enzymol.* **1996**, *1298*, 102–108; c) Y. Sugita, M. Nagai, Y. Yoneyama, *J. Biol. Chem.* **1971**, *246*, 383–388.

[21] a) E. H. Strickland, *Crit. Rev. Biochem.* **1974**, *2*, 113–175; b) I. Sirangelo, E. Bismuto, S. Tavassi, G. Irace, *Eur. Biophys. J.* **1998**, *27*, 27–31.

[22] a) A. Sulkowska, *J. Mol. Struct.* **2002**, *614*, 227–232; b) Y. Q. Wang, H. M. Zhang, G. C. Zhang, Q. H. Zhou, Z. H. Fei, Z. T. Liu, Z. X. Li , *J. Mol. Struct.* **2008**, *886*, 77–84.

[23] a) D. Silva, C. M. Cortez, J. C. Bastos, *Toxicol. Lett.* **2004**, *147*, 53–61; b) A. Q. Gong, X. S. Zhu, Y. Y. Hu, S. H. Yu, *Talanta* **2007**, *73*, 668–673; c) M. Ranjan, P. Diffley, G. Stephen, D. Price, T. J. Walton, R. P. Newton, *Life Sci.* **2002**, *71*, 115–126; d) Y. M. Huang, Z. J. Zhang, D. J. Zhang, J. G. Lv, *Talanta* **2001**, *53*, 835–841; e) D. Silva, C. M. Cortez, S. R. W. Louro, *Spectrochim. Acta Part A* **2004**, *60*, 1215–1223; f) J. R. Lakowicz in *Principles of Fluorescence Spectroscopy*, 2nd ed., Plenum Press, New York, **1999**, pp. 237–321.

[24] I. M. Klotz, *Ann. N. Y. Acad. Sci.* **1973**, *226*, 18–35.

[25] M. S. Kent, H. Yim, D. Y. Sasaki, J. Majewski, G. S. Smith, K. Shin, S. Satija, B. M. Ocko, *Langmuir* **2002**, *18*, 3754–3757.

[26] a) J. B. F. Lloyd, *Nature Phys. Sci.* **1971**, *231*, 64–65; b) W. C. Abert, W. M. Gregory, G. S. Allan, *Anal. Biochem.* **1993**, *213*, 407–413.

[27] E. A. Burstein, N. S. Vederkonra, M. N. Ivkova, *Photochem. Photobiol.* **1973**, *18*, 263–279.

[28] a) Y. Z. Zhang, B. Zhou, Y. X. Liu, C. X. Zhou, X. L. Ding, Y. Liu, *J. Fluoresc.* **2008**, *18*, 109–118; b) P. Mandal, T. Ganguly, *J. Phys. Chem. B* **2009**, *113*, 14904–14913.

[29] a) K. Nakashima, K. Yuda, Y. Ozaki, I. Noda, *Appl. Spectrosc.* **2003**, *57*, 1381–1385; b) M. O. Dayhoff, L. T. Hunt, P. J. McLaughline, D. D. Jones in *Atlas of Protein Sequence and Structure, Vol. 5* (Eds.: M. O. Dayhoff), National Biomedical Research Foundation, Baltimore, **1976**, Supplement 2, p. 208.

[30] H. D. Smith, Jr., C. O. Obenland, S. Papetti, *Inorg. Chem.* **1966**, *5*, 1013–1015.

Received: March 9, 2010
Published online: June 22, 2010

